Monitoring of surface water quality in large rivers with satellite imagery - Application to the Amazon basin

J.M. Martinez[1], J.L. Guyot[1], G. Cochonneau[1],

[1]Institut de Recherche pour le Développement (IRD), LMTG, Université Paul Sabatier, 14 Avenue Edouard Belin, 31 400 Toulouse, France Tel : (33) 5 61 33 26 72 - Fax : (33) 5 61 33 25 60 E-mail : martinez@ird.fr

ABSTRACT

Monitoring river water quality with satellite data has been limited by the lack of sensors offering high revisit frequency and suitable spatial and radiometric resolutions. In this communcation, it is shown that the last generation of moderate resolution sensors makes possible to monitor efficiently large tropical basins characterized by reduced field monitoring and strong cloud coverage. Emphasis is placed on monitoring suspended sediment concentration (SSC) at the river surface and we use a water quality database available for different locations along the Amazon River in Brazil and Peru. Six years of satellite data (MODIS) are reviewed and in particular, the 250 and 500-meter surface reflectance products are considered. It is shown that MODIS coarse resolution results in significant spectral mixing between river stream pixels and river sides covered by vegetation or sand banks. An automated reflectance retrieval algorithm has been developed to assess the water endmember pixels. The retrieved reflectance allows the seasonal cycle of the SSC to be reliably monitored along the Amazon River. Using the field measurement database for validation purposes, the SSC retrieval performance can be assessed. Prediction error of the SSC lies between 40 and 60 % depending on the site considered. The retrieval performance is reviewed as a function of MODIS product resolution, site dependence and river width for the whole 2000-2006 period.

1. INTRODUCTION

Usually, water quality monitoring in rivers is based on stations in the river streams where frequent samples are needed to characterize the variations in chemical and sediment concentrations that occur during the year, particularly between low and high flows and the different seasons of a year. These samples make it possible to determine reliably the material fluxes (the transport of a mass per unit time expressed as tons / year) by multiplying the concentration of a constituent by the stream discharge. Then, these material fluxes can be compared between stations to assess gains or losses or to compute the amounts of materials delivered to a reservoir or estuary. The ability to determine values such as source, transport, and delivery of constituents allows broad range of scientific and environmental policy issues to be addressed (Hooper 1997).

It is generally accepted that the state of the world's inland waters has to be better known. Indeed, three quarters of the world cannot afford the full-scale water quality monitoring infrastructure needed and will not be able to get it in the near future (GEMS 2003). The effectiveness and precision of follow-up is directly a function of the volume of measured data (quantity of stations, temporal sampling and number of parameters). However, the huge costs of maintining and managing networks have had a limiting effect on the number of stations installed. For example, in developed countries, faced with budget constraints, the number of samples collected at stations has diminished as a result of decreased sampling frequency and discontinuation of stations. Moreover, the quality of hydrologic data may vary greatly (e.g. sampling protocol) between watersheds and/or countries. As a result, these data cannot be easily used in studies at the global or regional scale.

Because conventional inland water monitoring techniques cannot catch up with the increasing demand for monitoring the impact of local and global changes, alternative solutions are required. Satellites can provide the synoptic, continuous and long-term global observation needed but owing to the characteristics of river systems specific satellite configuration are required. Hence, river systems exhibit four main specificities : 1) high temporal variability (i.e. the hydrologic regime) requiring a high revisit frequency; 2) a drainage network over large areas demanding a large spatial coverage; 3) narrow streams from a few tenths of meters up to a few kilometers for the largest rivers requiring an adequate spatial resolution; 4) complex optical properties of the inland waters in relation to clear oceanic waters due to organic and inorganic components at high concentrations calling for a fine radiometric resolution (number of bands and bandwidth).

Unfortunately, most past and present satellites are unsuited to water quality monitoring in rivers and lakes because these sensors fail to offer an adequate trade off between spatial resolution / spatial coverage / revisit frequency and radiometric resolution. As a result, the greater part of the works linking remote sensing data and some inland water quality parameters has been reduced to one-shot studies making use of high resolution imagery (A.G. Dekker 2002; Aranuvachapun and Walling 1988; Dekker and Malthus 1991; Doxaran et al. 2002; Mertes et al. 1993; Ritchie et al. 1987) or airborne sensors (Hakvoort et al. 2002; Robinson et al. 1998; Thiemann and Kaufmann 2002). However, some of the last generation spaceborne sensors and future satellite constellations seem promising in terms of inland water monitoring because they offer spatial resolution and spatial coverage which is now compatible with the dimensions of river systems while allowing for fine temporal revisit.

The primary purpose of this research work was to investigate the feasibility of using Moderate-Resolution Image Spectroradiometer (MODIS) surface reflectance data to identify variations in water color at the river surface on weekly and annual time steps. In particular we intend to determine the robustness of remote sensing reflectance as a predictor for some parameters of the water quality of continental waters. This research effort focused on monitoring suspended sediment load that encompasses a wide range of applications from contaminant transport (trace elements, nutrients, and hydrophobic organic compounds) (Martin and Windom 1991; Mayer et al. 1998), to water quality trends, reservoir sedimentation, lake eutrophication and/or soil erosion. Previous studies have shown that radiometric calibration of MODIS 250-m data (originally designed for land use) may be sufficiently accurate for TSS monitoring over turbid waters (Chen et al. 2007; Hu et al. 2004; Miller and McKee 2004) provided the TSS concentrations may be sufficiently high enough, of about 80 mg/l (Hu et al. 2004). Emphasis has been placed in this study on several methodological issues including the influence of watershed geomorphologic characteristics (river width, sediment type) and image acquisition (spatial resolutiont) on retrieval accuracy. The Amazon basin has been selected since it provides a large database of field measurements collected over several years in various stations located several hundreds of kilometers away from one another. Moreover, the Amazonian rivers present a large variety of characteristics in terms of river width (from a few hundred meters to several kilometers) and water types. Hence, the Amazon basin is ideally suited for detailed sensitivity analyses of remote sensing data.

2. STUDY AREA

The Amazon River is the widest river in the world, with an average discharge estimated at 209.000 m³/s in the estuary. The Amazon basin covers an area of about 6.4 millions km², extending between the Guyana Shield to the North and the Brazilian Shield to the South and the Andean and sub-Andean regions to the west. Figure 1 shows the Amazon mainstream that is formed by the Ucayali and Maranõn Rivers in the Peruvian Andes called Solimões River downstream the Brazilian boundary, changing to the Amazon River after its confluence with the Rio Negro. Three types of water are common throughout the Amazon River basin: white water, black water, and clear water (Sioli 1975). In the upper part of the basin the main tributaries of the Amazon River are generally white waters that are turbulent and brown because of the vast amount of nutrient-rich sediment carried from the Andes. The Negro River water are “black” originating in the lowest Amazonian terrain and wetlands that generally are dominated by podzol soils, they are loaded with organic material in colloidal suspension that give them their dark color At Iquitos, 3600 meters from the Atlantic Ocean, the river level is about 80 meters above the sea and at the confluence with the Negro river (in Manaus outskirsts), 1500 km from the sea, it is only 23 meters above the sea level. Two hundred kilometers downstream the Solimões-Negro confluence, the Amazon River receives the Madeira River waters, volumetrically the largest tributary and which contributes for about 50 % of the total solid fluxes of the Amazon River at its mouth in the Atlantic Ocean. Numerous smaller tributaries drain exclusively lowland regions into the river channels or into the floodplain.

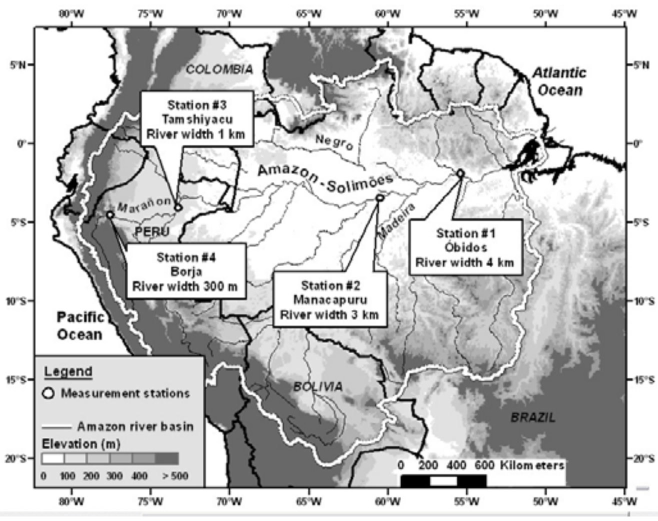

Figure 1. The Amazon basin and the location of the four river stations that are studied in this paper and for which ground measurements are available from the ORE-HYBAM network.

Suspended sediments at the Amazon River surface are mainly silt and clay particles. Studies have reported low particulate organic carbon (POC) content (1-4 % in terms of weight percentages relatively to the TSS concentration) in white water rivers (Ertel et al. 1986; Hedges et al. 1986; Moreira-Turcq et al. 2003). It has been shown that the POC concentrations vary directly with discharge and that the higher concentrations are reached during high water periods. These studies have pointed out that the DOC concentration show low seasonal difference in the mainstem of the river. Overall, the mean annual POC and DOC fluxes account for approximatively 20 % and 80 % respectively of the total carbon exported to the ocean by the Amazon River. A recent work (Guyot et al. 2007) has demonstrated that the sediment clay mineral composition highlights the evolution of the Amazon River, which starts in the Andes with high illite+chlorite content. On the other hand, clays from all the rivers draining the Guiana and the Brazilian shields present a typical clay assemblage with high kaolinite content, up to 100% in some rivers. In spite of the large spatial extent of these shield basins, the kaolinite content in the Amazon main stem remains low because of the very low sediment load delivered by these basins. Flowing into the Amazon floodplain, the Andean rivers show a significant enrichment in smectite, provided by lateral bank erosion as suggested by Johnsson and Meade (1990). In Brazil the Amazon River sediment presents a clay assemblage (mainly smectite) that is not typically Andean.

3 DATA

The Collection 4 atmospherically-corrected surface reflectance products from Terra and Aqua MODIS sensors are utilized in this study. The MODIS data product MOD09Q1 provides calibrated reflectance for two bands measured at 250 m pixel resolution (http://modis.gsfc.nasa.gov). Band 1 is centered at 645 nm and band 2 at 858.5 nm. MOD09A1 provides calibrated reflectance for seven spectral bands in the 400–2500 nm spectral region measured at 500 m pixel resolutions. MODIS surface reflectance 8-day composite data in HDF format was acquired between February 2000 and January 2007 from the NASA Earth Observing System (EOS) data gateway. Four time series of data (250-meter and 500-meter products for both Terra and Aqua MODIS sensors) were chosen to analyze temporal variations of the reflectance through the seasonal cycle. We chose composite images because 1) the 8-day composite is compatible with the 10-day field measurement sampling frequency; 2) it reduces the amount of data to analyze as a large number of daily images cannot be used in view of the persistent cloud cover; 3) it significantly reduces the BRDF and atmospheric artifacts. Figure 2 shows MODIS 250-meter 8-day composites over the four measurement stations considered here (see section 4.2).

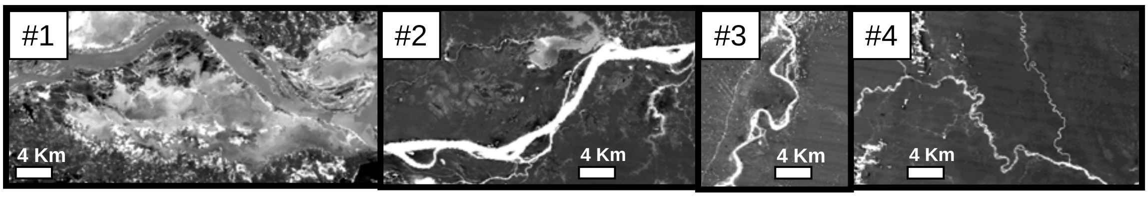

Figure 2 : MODIS images acquired over the four river stations understudy : #1 Obidos (Brazil, 700 km from the Ocean); #2 Manacapuru (Brazil, 1300 km from the Ocean); #3 Tamshiyacu (Peru, 3200 km from the Ocean) and #4 Borja (Peru, 3800 km from the Ocean).

4 METHOD

4.1 RETRIEVAL OF SURFACE REFLECTANCE OVER RIVER STREAMS

Data analysis shows that the retrieval of river stream reflectance using MODIS data is hampered by the low spatial resolution that may result in few (or no) pure (non-mixed) water pixels depending on river width. Figure 3 illustrates this phenomenon with different scatterplots of MOD09Q1 pixels from a river mask applied over two stations along the Amazon River at different dates. In station #1 (Obidos) the Amazon River is 4 kilometer-wide, while in #3 it is only 1 kilometer wide. Pixels corresponding to clouds or where atmospheric correction has not been processed were first removed using MODIS quality band. Analysis of these scatterplots makes it possible to assess the spectral mixing in each image. Spectrally pure pixels are found at the vertices of the polygon or line that binds the data space.

Theoretically, if all pixels lie within the polygon or on the line formed by endmembers, the mixture model can be considered an ideal linear model. The clear delineation of feature spaces corresponding to the red and NIR channels (Fig. 3) suggests that the reflectance spectra of the MODIS image might best be represented by one (figure 3a), two (figures 3b and 3d) or three endmembers (figures 3c and 3e) depending on each acquisition. In Figures 3b and 3d, vegetation endmember is clearly separated with a strong NIR reflectance and a low red reflectance. White water endmember appears at the other extreme end of Figure 3b with moderate reflectance values in the red and lower NIR channels. In Figures 3c and 3e, another endmember appears with high albedo pixels that have a far larger variability and correspond to sand banks or unfiltered cloud borders.

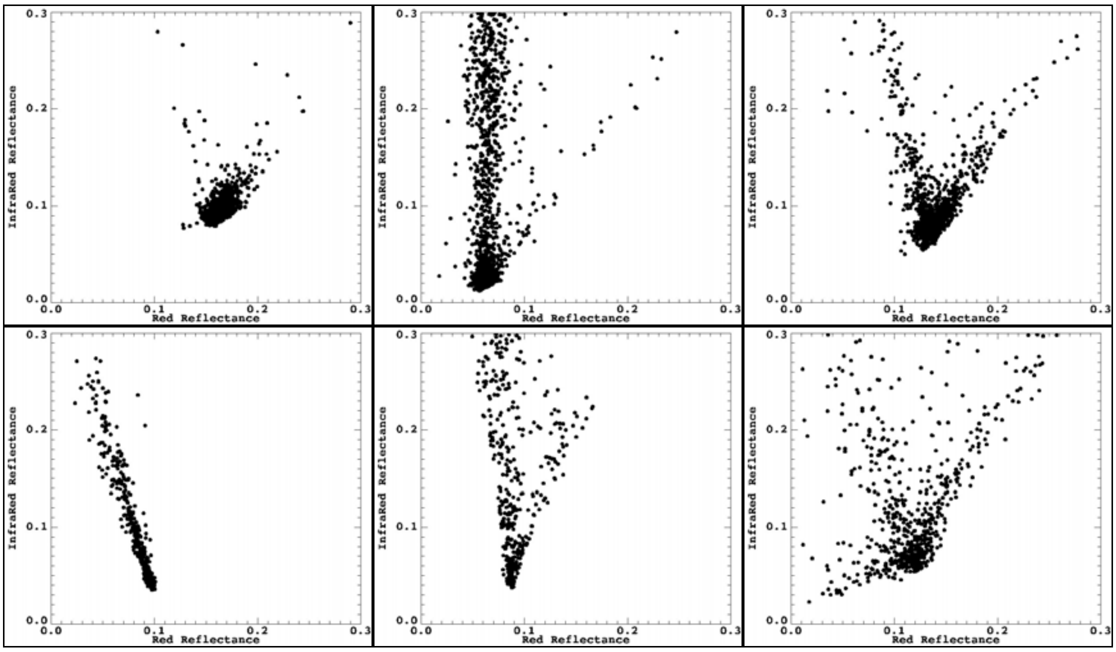

Figure 3. Surface reflectance values (MOD09Q1 products) for MODIS band 1 and 2 over the Amazon river for stations #1 and #3 and 3 dates.

Of particular interest, spectral mixing appears to vary temporally depending on 3 factors : 1) river hydrology (depending on river water level, river width may vary and some sand banks may emerge and greatly affect the resulting spectral signature); 2) the variation of the MODIS effective resolution that is degraded at high view zenith angles because individual observations cover several adjacent grid cells at high view zenith angles (Justice et al. 2002); 3) the presence of some local residual atmospheric effects. In other words, it is impossible to retrieve geometrically pure water pixels from pixel-based mask and we need to develop a specific retrieval procedure to assess the river water endmember in each image.

The methodology for getting estimates of the river water endmember from MODIS images is organized in four steps. Firstly, pixels are extracted over the river from each image using a pixel-based mask designed for the whole time series. Secondly, the pixels are partitioned into homogeneous clusters using K-means algorithm. Thirdly, vegetation endmember as well as high and low albedo endmembers are retrieved using the same MODIS scene. Fourthly, different linear mixing models (LMM) are tested using either 2, 3 or 4 endmembers. This procedure essentially focuses on the autonomous determination of the water end-member by successive testing of each pixel cluster in each LMM to find the cluster that best describe the remaining groups of mixed water pixels over the river stream. The pixel cluster leading to the lowest residual among the different LMM´s is retained as water endmember. More information can be found in Martinez et al. paper (2007)

The methodology relies on two assumptions : (1) spatial resolution in relation to river width is fine enough to get effectively “pure” water pixels in the scene; (2) radiometric calibration and atmospheric corrections are accurate enough to compare reflectance values in space and time. The first assumption as well as the quality of the water endmember estimates can be checked *a posteriori* by analyzing the retrieved water endmember spectral signature (both mean and variance) against referenced white water spectra. For example, spectroradiometric field measurements show that reflectance of white water always decreases from red to infrared owing to the strong light absorption by the water in the infrared domain. Thus, if the IR reflectance of the water endmember estimate is higher than the reflectance in the red channel, the water endmember is likely to be invalid. Such spectral irregularity is typical of a spectral mixing between water and vegetation characterized by a strong infrared reflectance. Then, if spectral signature is considered invalid or exhibiting a large variance, the estimate is rejected and the processing moves to the next image in the time series. The second assumption is likely to be respected as it is largely accepted that the MODIS sensors have good radiometric performance (Chen et al. 2007).

4.2 VALIDATION

Figure 1 shows the four locations along the Amazon river and its main tributaries for which we have time series of SSC measurements at the river surface from the Environmental Research Observatory (ORE) HYBAM (Geodynamical, hydrological and biogeochemical control of erosion/alteration and material transport in the Amazon basin). HYBAM provides the research community with the high quality scientific data needed to understand and model the Amazon system behavior and their long-term dynamics. HYBAM also collaborates with local institutions of the Amazon basin (national agencies and universities) to insure the sustainability of the observation data. HYBAM is operating with measurements and samplings at different time intervals (from daily sampling for water level to monthly sampling for geochemical parameters or isotopes, and ten-days interval sampling for suspended material), regular control visits at the measurement stations, sample analysis in laboratories, validation of the data and updating of the geo-referenced database. Suspended sediment concentration at the river surface is sampled at each station from a small boat every 10 days on a fixed point with 250-ml sampling bottle. Samples are collected in acid-cleaned high density polyethylene (HDPE) containers and filtered immediately through 0.22 µm Millipore® membranes, previously dried during 24 hours at 50°C and weighted. At the laboratory, membranes are dried and weighted to obtain the amount of suspended matter by unit of liquid. Because cloud free MODIS images rarely match the field measurement date, linear interpolation is used between 10-day SSC measurements to produce daily SSC time series. Then the interpolated data is used and compared with MODIS surface reflectance data.

The HYBAM stations under study were selected to offer increasing river width and lower temporal variability from upstream to downstream. Figure 4 shows the daily water levels recorded during 2005 at the four stations. It can be seen that the river shows progressively a regular monomodal flood pattern together with a decreasing temporal variability from upstream to downstream. The SSC is strongly correlated with the runoff upstream but becomes partially decorrelated downstream. The four stations studied are Borja, Tamshiyacu, Manacapuru and Obidos. Figure 3 shows 250-meter MODIS images over each station. Borja (station #4) is located in the piedmont of the Andes, after the confluence of the Marañon and

Santiago rivers in Peru. The river width varies roughly from 200 to 450 meters in the vicinity of the station. Formally, the union of the Ucayali and the Marañon rivers forms the Rio Amazonas, which changes its name to Solimões on the triple frontier between Peru, Columbia and Brazil, and later changes its name back to the Amazon only after it meets the Rio Negro near Manaus. Tamshiyacu (station #3) is located downstream the confluence of Marañon and Ucayali rivers at an altitude of 65 meters. The Amazon River at Tamshiyacu presents a mean discharge of 43.000 m^3/s and the river width is of about 1000 meters. Manacapuru (station #2) is located in the central Amazon plain in Brazil where the Solimões have a discharge of about 100.000 m^3/s. The river width at Manacapuru varies between 2000 and 4000 meters. Finally, Obidos (station #1) is located 900-kilometer upstream from the Amazon river mouth with a mean discharge of about 200.000 m^3/s and a river width varying between 2000 and 4000 meters.

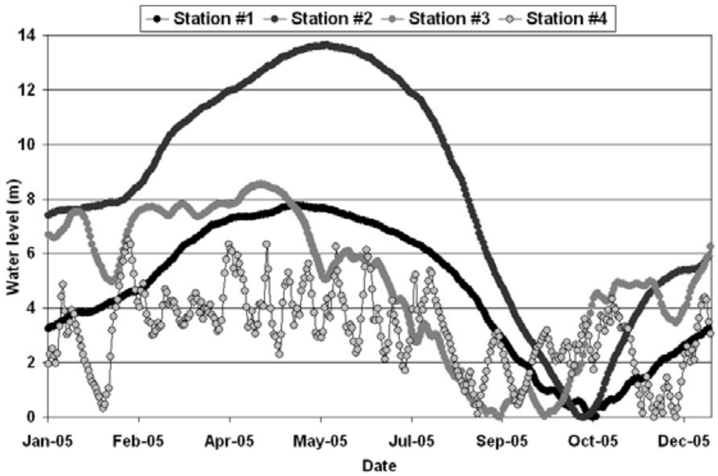

Figure 4 : Variation of daily water levels recorded at the four stations understudy during 2005. For clarity, the water level minimum recorded at each station has been set to 0. Water level range increases downstream to upstream (station #4 to station #2). On the contrary the hydrological variability is much stronger upstream (station #4) in relation to the reduced catchment size while the Amazon River exhibits a well defined monomodal flood downstream (stations #1 and 2).

The ORE-HYBAM data provides unprecedented knowledge of the temporal behavior of SSC concentrations along the Amazon River. However the comparison of field data and MODIS estimates in uneasy provided that both estimates are not assessed over the same area. While MODIS reflectance will be assessed on hundreds of pixels, the field data consists of pointwise estimates. Moreover, the ORE-HYBAM data provides SSC estimates but no error bars. In order to quantify the mean error associated with the ORE-HYBAM 10-day estimates, we conducted two field experiments at station #2 to link the point wise estimates to data acquired simultaneously on a larger grid across the river reach at the same station.

5 RESULTS

5.1 REFLECTANCE TEMPORAL BEHAVIOR

We analyze the temporal behavior of the river water endmenber reflectance in relation to ground measurements. Figure 5 compares the IR surface reflectance time series extracted automatically from MODIS Terra 250m products with SSC time series for the four stations.

The SSC presents a well-defined annual cycle in relation to the monomodal flood of the main Amazonian rivers with higher concentrations during the increasing water period (the concentration peak always occurs a few weeks before the flood peak) and lower concentrations during the decreasing water period. However, the seasonal cycle is less pronounced upstream and at station #4 we observe a much stronger variability between 10-day consecutive samples. Direct comparisons of field measurements and MODIS data are difficult because spatial and temporal samplings are extremely different. On the one hand, a 250-ml sample is taken each 10 days on a fixed point. On the other hand, we retrieve the reflectance the MODIS on a much wider area (from hundreds to thousands of pixels) and with a temporal sampling depending on the local meteorology. Yet, we note that there is a general good agreement between the ground measurements and the reflectance and that the annual cycle is well-monitored by satellite data with correct timing. The automatic retrieval procedure appears to produce robust estimates over the 7 consecutive hydrological cycles of the Amazon River..

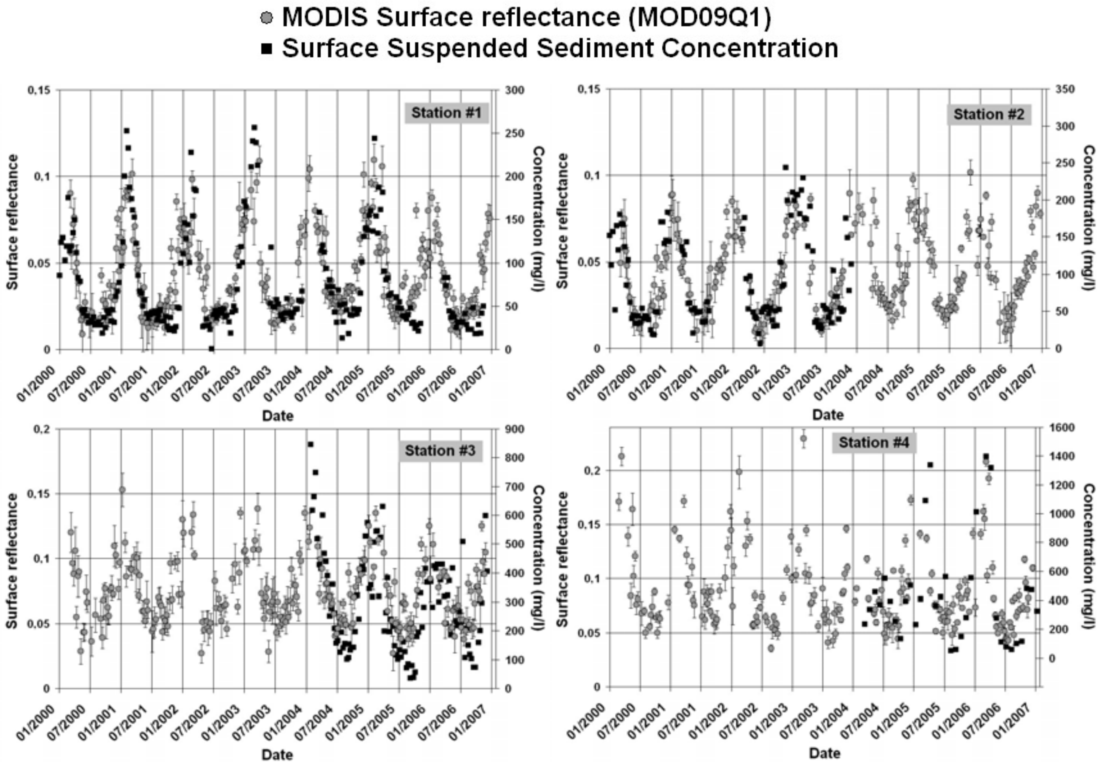

Figure 5. Comparisons of water endmember reflectance time series (250-meter Terra images) with 10-day SSC field measurements over the 2000-2006 period at stations #1,#2,#3 and #4 along the Amazon river.

5.2 SSC RETRIEVAL

Numerous works have studied the sensitivity of remote sensing reflectance to the suspended sediment concentration in oceanic and inland waters. A significant number of researchers have reported a strong positive correlation between SSC and spectral radiance (Bhargava and Mariam 1990, 1991; Doxaran et al. 2002; Hinton 1991; Novo et al. 1989a, b; Ritchie and Cooper 1988; Ritchie et al. 1987) and also noted that the relation may depend on the range of concentration, water types and suspended matter origin. Most studies agree that the best correlation between reflectance and SSC is between 700 and 800 nm in turbid inland waters.

Figure 6 presents the variation of reflectance for the MODIS MOD09Q1 product, band 2, as a function of SSC concentrations using all the reflectance data and corresponding SSC estimates we had for the four stations. Surface Suspended Concentrations present a wide range of values from 18 mg/l up to 1550 mg/l. There is a significant positive correlation between field data and surface reflectance. The relationship is more particularly remarkable as data originates from different years (from 2000 to 2006) and has been acquired in different stations located thousands of kilometers away from one another. The accuracy of the relationship between surface reflectance and SSC concentrations has been assessed using the Bootstrap technique and power-law model. The general bootstrap approach involves resampling of the dataset (SSC and reflectance) with repeated replacements (Wehrens et al. 2000) to generate an empirical estimate of the sampling distribution. Accordingly, a large number of 'bootstrap samples' is generated, each of the same size as the original dataset. To achieve a better estimate of the prediction error, we use the *0.632 bootstrap* b_{632}. Practical and theoretical evidence suggests that this is a very reliable estimator (Efron and Tibshirani 1993). The dataset for regression and validation consists of 414 SSC estimates, from 16 to 1537 mg/l with a mean value of 144 mg/l. Figure 7 shows the measured vs satellite-derived SSC using power-law model and bootstrap resampling technique. The b_{632} estimate is 123 mg/l (86 % relative error). Accuracy of the SSC retrieval is adequate for monitoring given the major spatial scale difference between in-situ measurements (250-millimeter samples) and the reflectance data (assessed from buffers containing hundreds of pixels). However, a significant dispersion may be related to different factors such as : 1) site dependence; 2) reflectance variability introduced by miscalibration or adjacency effects; 3) temporal dependency of the reflectance – SSC relationship. To analyze the impact of these different error sources a closer look at the dataset is now considered.

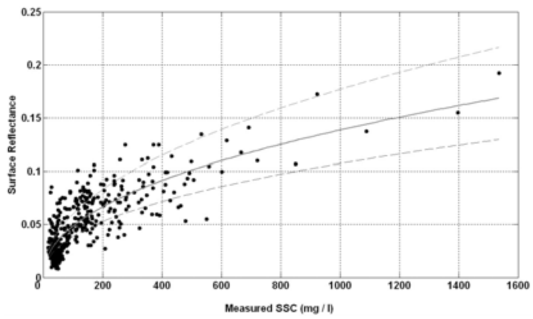

Figure 6 : Comparison of reflectance extracted from MODIS images (Terra 250-meter infrared band) with field measurements acquired on the same period over four stations (see Figure 1).

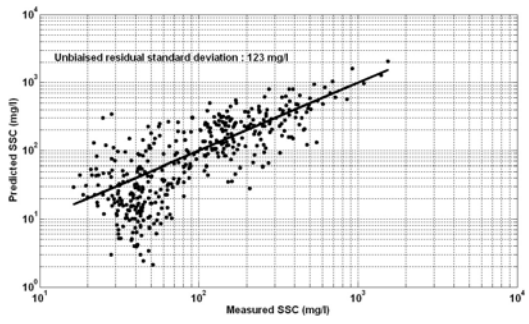

Figure 7 : SSC daily estimates from the ORE HYBAM versus surface reflectance extracted from MODIS Terra 250-meter infrared band over four stations (see Figure 1).

5.3 INFLUENCE OF THE SEDIMENT MATERIAL PROPERTIES

Kirk (1994) states that the quest for a universal algorithm for suspended sediments is never likely to succeed no matter what combination is used because the scattering efficiency of suspended particles per unit weight is very much a function of size and average particle size of sediments is quite variable both with time and place. Experimental measurements in the laboratory have confirmed this statement by analyzing the scattering and absorption properties of different marked sediment types (Babin and Stramski 2004; Han and Rundquist 1996; Novo et al. 1989a). Because the sediment type varies significantly from one station to another (see Study Area section) the Amazon River appears very appropriate to infer the impact of the sediment properties on reflectance. A robust linear relationship is established between band 2 MODIS Terra 250 m data and in situ measurements of TSS at each station and we compare statistically the SSC / reflectance relationship parameters computed for each station. It is found that the slope of the linear model is different between stations #1 and #2 ($p = 0.005$) but that the intercept is similar ($p= 0.4$). Also, a significant statistical difference occurs between station #3 and station #4 ($p = 0.005$ for both slope and intercept).

Then, the retrieval performance is assessed for each station using the b_{632} estimate to quantify the SSC prediction error from the model. To do this, we use all points available in each station acquired between 2000 and 2006. At station #1, the relative prediction error (b_{632} estimate) using MODIS Terra 250-meter IR channel is 49 % (N = 207, absolute prediction error : 33 mg/l). At station #2, the relative prediction error falls to 41 % (N = 108, absolute prediction error : 33 mg/l). This should be considered as quite significant because intensive field sampling have shown (Martinez et al. 2007) that a prediction error less than 50 % cannot be expected when compared to 10-day field measurements. At station #3, we note a lower performance with a prediction error of 59 % (N = 107, absolute prediction error : 145 mg/l). At this station, the SSC range is much greater than in the two first stations and the assumption of a linear relationship between SSC and reflectance over this range is not fulfilled. At station #4, the retrieval prediction error reaches 53 % (N = 29, absolute prediction : 248 mg/l). For this station, the SSC / reflectance relationship was computed using monthly averaged data because the temporal variability is so strong that comparisons of individual estimates acquired at different days no longer make any sense. These findings support the view that a better retrieval performance is achieved if the dataset is partitioned per station.

As suggested by Kirk, significant site dependence can be observed between surface reflectance and SSC. However these differences evidence real modifications in the sediment mineralogy between stations, as suggested by Guyot et al. (2007). At station #4 the Marañón River exhibits a dominant illite+chlorite clay assemblage (53%) and significant smectite content (17%) (Guyot et al. 2007). At station #3, the Amazon River presents an intermediate clay assemblage between the Marañón and Ucayali rivers. The clay assemblage is richer in smectite than in the Marañon River. Downstream, at station #2 the Solimões River shows a clay assemblage with a much higher smectite content (57 %). At station #1, the Amazon River presents a clay mineral assemblage similar to a mixing of Madeira and Solimões rivers, with smectite accounting for approximatively 50%, illite and chlorite, 30% and kaolinite 20% (Guyot et al. 2007). The reflectance / SSC relationship is clearly affected by the upstream/downstream sediment type gradient. Also worth noticing is the high temporal stability that makes it possible to consider a long term monitoring of SSC from space. However, SSC monitoring using satellite data would benefit from field observations to help define homogeneous reaches of the river where a unique reflectance / SSC relationship could be applied. These findings underscore the need for a joint analysis of field data and remote sensing images to produce reliable estimates of water quality parameters.

5.4 INFLUENCE OF SENSOR SPATIAL RESOLUTION

The impact of sensor spatial resolution has been investigated by assessing 1) for each resolution mode the accuracy of the SSC retrieval using b_{632} estimate for prediction error; 2) whether the model parameters of the SSC / reflectance relationship (linear model) are statistically different between both modes. The retrieval performance is assessed separately in each station and for decreasing river widths from station #1 (4 km wide), station #2 (2 km wide) to station #3 (1 km wide). In station #1, the relationship between surface reflectance and SSC concentrations is similar for both resolutions ($p = 0.25$ and $p = 0.4$ for slope and intercept respectively). Accordingly, the retrieval accuracy using the bootstrap techniques shows close performances with a prediction error (b_{632}) of 33.1 mg/l between predicted and measured SSC (49 % relative error with N = 222) for the 250-meter resolution mode and b_{632} =32.9 mg/l (49 % relative error with N = 199) for the 500-meter resolution mode. It is worthwhile noting that the number of validation samples for each resolution mode is different because we do not have 500-meter 8-day composites for the year 2000. For this station, the river width is significantly larger than the pixel size. Therefore it appears that there is no significant dependence of the SSC retrieval on the MODIS resolution.

In station #2, the relationship between surface reflectance and SSC concentrations is similar in both resolutions ($p = 0.4$ for slope and intercept). Accordingly, the retrieval accuracy is almost similar with 33.5 mg/l of error between predicted and measured SSC (41 % relative error with N = 84) for the 250-meter resolution mode and 25.9 mg/l of error (37 % relative error with N = 59) for the 500-meter resolution mode. The difference in accuracy values between both resolution modes is induced by the different number of points available for validation : 59 points for the 500-meter resolution mode and 84 for the 250-meter resolution mode. As in station #1, this is due to the absence of 500-meter image composites for year 2000. Again, there is no significant dependence of the SSC retrieval on the MODIS resolution.

In station #3, the relationship between surface reflectance and SSC concentrations shows some differences even though it not possible to exclude the similarity in both resolutions ($p = 0.025$ and $p = 0.25$ for slope and intercept respectively). The retrieval accuracy is slightly different : the retrieval error is 145.8 mg/l (59 % relative error with N = 96) for the 250-meter resolution mode and 126.0 mg/l error (51 % relative error with N = 64) for the 500-meter resolution mode. This difference in accuracy is due to the different numbers of validation dates between both resolution modes that introduce a slight variability in the subsequent validation estimates. Unlike stations #1 and #2 this difference is not due to the unavailability of 500-meter image composite for year 2000. We cannot retrieve water endmember reflectance in 17 % of the cases (44 out of 272 8-day composite images) for the 250-meter resolution mode because of strong cloud coverage. For the 500-meter resolution mode, this rate increases to 36 %. This difference is likely to be caused by the degradation of MODIS effective resolution at high view zenith angles which makes that it occurs more frequently that pure water pixels cannot be find in 500-meter scenes than in 250-meter scenes. Hence, for a river width of 1 km, the influence of the river width induces slight differences in the SSC retrieval even though we cannot conclude statistically on a difference. Yet, we observe that the use of 500-meter images leads to a higher rejection rate of the MODIS images. We do not have measurement stations presenting river width between 500 meters and 1-kilometer.

However, we can infer from the results obtained over station #3 that a river width that is twice the image resolution is a threshold beneath which the retrieval accuracy may be affected.

6 CONCLUSIONS

The objective of the paper was to investigate the feasibility of using MODIS surface reflectance data to identify variation in water color at the river surface on weekly and annual time frames. Our results suggest that the medium spatial resolution does not preclude the use of sensors such as MODIS for monitoring the world's largest rivers. In particular, the surface reflectance data appears to be robustly linked with some water quality parameters such as SSC. However it is shown that reflectance retrieval is not easy over rivers because the coarse spatial resolution induces spectral mixing. Furthermore, the spectral mixing is shown to be changing depending on hydrological factors (river width controlled by flood stage, presence of sand banks) and acquisition geometry (depending on MODIS imaging angle). Accordingly, a specific algorithm has been developed for water endmember retrieval among the pixels extracted over the river stream. The core of this procedure lies in the autonomous determination of the water end-member by successively testing each pixel cluster over the river stream with different linear mixing models to find the cluster that can be used to describe at best the remaining groups of mixed water pixels. By using the information present in each image and *a priori* limited knowledge (i.e. vegetation, low and high albedo endmembers are directly retrieved within each image) the algorithm makes full use of the parameters available in the multitemporal dataset. This procedure has demonstrated its ability to provide robust estimates of the water reflectance over seven consecutive hydrological cycles and for river reaches along the Amazon River presenting marked differences in terms of SSC range, river width or mineral composition.

In terms of general guidelines, it is shown that MODIS can be used for SSC monitoring of rivers larger than 500 meters. On the one hand, a minor but significant site dependence can be observed in the SSC / reflectance relationship following sediment composition variation. On the other hand, a strong temporal robustness can be found in the SSC / reflectance relationship when each station along the river is considered separately. Hence, our study shows that it is now possible to get water quality parameter over rivers from medium resolution satellite for long term monitoring. By combining an excellent temporal resolution and a fine calibration quality MODIS paves the way for potentially rewarding remote sensing data applications to continental water monitoring. However more studies are needed to fully assess the retrieval accuracy of water quality parameters such as SSC. In particular, more robust inversion retrieval techniques will have to be developed using either statistical models or classical approaches based on the knowledge of water optical properties. The monitoring of the world's largest rivers will clearly benefit from such technological approach.

BIBLIOGRAPHY

A.G. Dekker, R.J.V., S.W.M. Peters (2002). Analytical algorithms for lake water TSM estimation for retrospective analyses of TM and SPOT sensor data. *International journal of remote sensing, 23*, 15-35

Aranuvachapun, S., & Walling, D.E. (1988). Landsat-MSS Radiance as a measure of suspended sediment in the lower Yellow River (Hwang Ho). *Remote Sensing of Environment, 25*, 145-165

Babin, M., & Stramski, D. (2004). Variations in the mass-specific absorption coefficient of mineral particles suspended in water. *Limnology and Oceanography, 49*, 756-767

Bhargava, D.S., & Mariam, D.W. (1990). Spectral refletance relationships to turbidity generated by different clay materials. *Photogrammetric Engineering Remote Sensing, 56*, 225-229

Bhargava, D.S., & Mariam, D.W. (1991). Effects of suspended particle size and concentration on reflectance measurements. *Photogrammetric Engineering Remote Sensing, 57*, 519-529

Chen, Z., Hu, C., & Muller-Karger, F. (2007). Monitoring turbidity in Tampa Bay using MODIS/Aqua 250-m imagery. *Remote Sensing of Environment*, *109*, 207-220

Dekker, G.A., & Malthus, T.J. (1991). Quantitative Modeling of Inland Water Quality for High-Resolution MSS Systems. *IEEE Transactions on Geoscience and Remote Sensing, 29*, 89-95

Doxaran, D., Froidefond, J.M., Lavender, S., & Castaing, P. (2002). Spectral signature of highly turbid waters. Application with SPOT data to quantify suspended particulate matter concentrations. *Remote Sensing of Environment, 81*, 149-161

Efron, B., & Tibshirani, R.J. (1993). *An introduction to the bootstrap*. New York

Ertel, J.R., Hedges, J.I., Devol, A.H., Richey, J.E., & Ribeiro, M.N.G. (1986). Dissolved humic substances of the Amazon River system. *Limnology and Oceanography, 31*, 739-754

GEMS (2003). Improving Global Water quality monitoring - Technical Advisory Paper No. 1. In: United Nation Environment Program - Global Environment Monitoring System

Guyot, J.L., Jouanneau, J.M., Soares, L., Boaventura, G.R., Maillet, N., & Lagane, C. (2007). Clay mineral composition of river sediments in the Amazon basin. *Catena, 71*, 340-356

Hakvoort, H., De Haan, J., Jordans, R., Vos, R., Peters, S., & Rijkeboer, M. (2002). Towards airborne remote sensing of water quality in the Netherlands - Validation and Error Analysis. *ISPRS Journal of Photogrammetry & Remote Sensing, 57*, 171-183

Han, L., & Rundquist, D.C. (1996). Spectral characterization of suspended sediments generated from two texture classes of clay soil. *International journal of remote sensing, 17*, 643-649

Hedges, J.I., Ertel, J.R., Quay, P.D., Grootes, P.M., Richey, J.E., Devol, A.H., Farwell, G.W., Schmidt, F.W., & Salati, E. (1986). Organic Carbon-14 in the Amazon River System. *Science, 231*, 1129-1131

Hinton, J.C. (1991). Application of eigenvector analysis to remote sensing of coastal water quality. *International journal of remote sensing, 12*, 1441-1460

Hooper, R.P. (1997). Sediment sampling in the national stream quality accounting network In, *US Geological Survey Sediment Workshop*

Hu, C., Chen, Z., Clayton, T.D., Swarzenski, P., Brock, J.C., & Muller-Karger, F.E. (2004). Assessment of estuarine water-quality indicators using MODIS medium-resolution bands: Initial results from Tampa Bay, FL. *Remote Sensing of Environment, 93*, 423-441

Johnsson, M.J., & Meade, R.H. (1990). Chemical weathering of fluvial sediments during alluvial storage: the Macuapanim island point bar, Solimoes River, Brazil. *Journal of Sedimentary Petrology, 60*, 827-842

Justice, C.O., Townshend, J.R.G., Vermote, E.F., Masuoka, E., Wolfe, R.E., Saleous, N., & al., e. (2002). An overview of MODIS land data processing and product status. *Remote Sensing of Environment, 83*, 3-15

Kirk, J.T.O. (1994). *Light and Photosynthesis in Aquatic Ecosystems*: Cambridge University Press

Martin, J.M., & Windom, H.L. (1991). Present and future roles of ocean margins in regulating marine biogeochemical cycles of trace elements. In R. Mantoura (Ed.), *Ocean margin processes in global change. Report, Dahlem workshop, Berlin, 1990* (pp. 45-67): Wiley

Martinez, J.M., Guyot, J.L., Cochonneau, G., Espinoza Villar, R., Filizola, N., & Seyler, F. (2007). Surface water quality monitoring of rivers with MODIS data - Application to the Amazon River. *Submitted to Remote Sensing of Environment*

Mayer, L.M., Keil, R.G., Macko, S.A., Joye, S.B., Ruttenberg, K.C., & Aller, R.C. (1998). The importance of suspended particulates in riverine delivery of bioavailable nitrogen to coastal zones. *Global Biogeochemical Cycles, 12*, 573-579

Mertes, L.A.K., Smith, C.T., & Adams, J.B. (1993). Estimating Suspended Sediment Concentrations in Surface Waters of the Amazon River Wetlands from Landsat Images. *Remote Sens.Environ., 43*, 281-301

Miller, R.L., & McKee, B.A. (2004). Using MODIS Terra 250 m imagery to map concentrations of total suspended matter in coastal waters. *Remote Sensing of Environment, 93*, 259-266

Moreira-Turcq, P., Seyler, P., Guyot, J.L., & Etcheber, H. (2003). Exportation of organic carbon from the Amazon River and its main tributaries. *Hydrological processes, 17*, 1329-1344

Novo, E.M.L.M., Hamsom, J.D., & Curran, P.J. (1989a). The effect of sediment type on the relationship between reflectance and suspended sediment concentrations. *International journal of remote sensing, 10*, 1283-1289

Novo, E.M.L.M., Hamsom, J.D., & Curran, P.J. (1989b). The effect of viewing geometry and wavelength on the relationship between reflectance and suspended sediment concentration. *International journal of remote sensing, 10*, 1357-1372

Ritchie, J.C., & Cooper, C.M. (1988). Comparison of measured suspended sediment concentrations with suspended sediment concentrations estimated from Landsat MSS data. *International journal of remote sensing, 9*, 379-387

Ritchie, J.C., Cooper, C.M., & Yongqing, J. (1987). Using Landsat Multispectral Scanner data to estimate suspended sediments in Moon Lake, Mississippi. *Remote Sensing of Environment, 23*, 65-81

Robinson, M.C., Morris, K.P., & Dyer, K.R. (1998). Deriving fluxes of suspended particulate matter in the Humber estuary, UK, using airborne remote sensing. *Marine Pollution Bulletin, 37*, 155-163

Sioli, H. (1975). Amazon tributaries and drainage basins. *Landscapes of river basins (South America)* (pp. 199-213). New York: Springer Verlag

Thiemann, S., & Kaufmann, H. (2002). Lake water quality monitoring using hyperspectral airborne data - a semiempirical multisensor and multitemporal approach for the Mecklenburg Lake District, Germany. *Remote Sensing of Environment, 81*, 228-237

Wehrens, R., Putter, H., & Buydens, L.M.C. (2000). The bootstrap: a tutorial. *Chemometrics and Intelligent Laboratory Systems, 54*, 35-52